COMADEM

International Journal of Condition Monitoring and Diagnostic Engineering Management

Effects of blade tapering on the performance of vertical axis wind turbines analysed through advanced visualization techniques

Martin Zahariev [a], Taimoor Asim [b*], Rakesh Mishra [c], Blaise Nsom [d]

[a] *Dronamics Ltd, Sofia 1729, Bulgaria*

[b] *School of Engineering, Robert Gordon University, Garthdee Road, Aberdeen, UK AB10 7GJ*

[c] *School of Computing and Engineering, University of Huddersfield, Queensgate, Huddersfield, UK HD1 3DH*

[d] *Université de Bretagne Occidentale, IUT de Brest, IRDL UMR CNRS 6027, France*

∗ *Corresponding author. Tel.: +44-1224-262457; email: t.asim@rgu.ac.uk*

ABSTRACT

Harnessing the wind energy effectively and efficiently, to fulfil the ever increasing energy demands, has long been an area of active research. This research study is aimed at exploring the blade design of a small-to-medium sized Savonius type Vertical Axis Wind Turbine (VAWT) for urban applications, as the published research in this area is severely limited. A commercial Computational Fluid Dynamics (CFD) based solver has been used to numerically simulate airflow around a conventional (cup-shaped) 2-bladed VAWT over a wide operational range (i.e. Tip Speed Ratio (TSR) from 0.4-1) in order to identify the peak performance point. Blade tapering has been shown to affect the performance of a wind turbine. As such, in the present study, three different VAWT configurations have been used with blade tapering corresponding to Delta, Rhomb and Cross shaped blades. It has been observed that tapering the blades of a Savonius VAWT significantly reduces the torque coefficient of the turbine, while there is a slight decrease in the power coefficient. Comparing the three tapered blade configurations, the delta blades depict higher performance than the competitor designs.

Keywords: *Vertical Axis Wind Turbine; Computational Fluid Dynamics; Tip Speed Ratio; Torque Coefficient.*

1. Introduction

Wind energy originates from the solar energy. The wind flow is caused by the uneven heating of the earth's surface by the sun. Wind energy can be harnessed using various types of mechanical artefacts. Wind turbines is one such machine that harnesses wind energy. There are many types of wind turbines, one of which is the Savonius type VAWT, or the drag based VAWT, named after Finnish engineer Sigurd Johannes Savonius. These VAWTs operate at lower TSRs. As these VAWTs operate under the principle of drag force application, the rotational speed of the turbine can rarely go above the wind speed, making the Savonius type VAWTs operate at lower speeds, yet yielding high torque. A VAWT's performance can be expressed in terms of its torque coefficient (Cm) and its power coefficient (Cp) as:

$$Cm = \frac{T}{\frac{1}{2}\rho ARV^2} \qquad (1)$$

$$Cp = \frac{T\omega}{\frac{1}{2}\rho AV^3} \qquad (2)$$

where T, A, R and ω are the torque output (Nm), the swept area (m^2), the radius (m) and the rotational speed (rad/sec) of VAWT's blades, while ρ and V are the density (kg/m^3) and velocity (m/sec) of air. It can be seen from equations (1-2) that the method of energy extraction in VAWTs is mainly defined by the way the blades interact with the incident air flow.

As tapered blade VAWTs have been shown in [1] to be better suited for urban environments due to their low start-up torque requirements, in the present study, various configurations of tapered blades have been considered for investigations in order to identify the optimal tapered blade design/s. For this purpose, a conventional Savonius type VAWT has been numerically modelled and analysed, using advanced Computational Fluid Dynamics (CFD) based techniques, to estimate its performance characteristics at a wide range of operation. Researchers around the world have been using CFD based techniques for flow diagnostics within a range of different flow handling systems [2-9]. The effects of blade tapering have been critically analysed at the peak efficiency point identified for the conventional VAWT design.

2. Methodology

The dimensionless ratios of the Savonius VAWT considered in the present study are the i) overlap ratio of 0.22, ii) gap ratio of 0.07 and iii) aspect ratio of 5. The end plates are 20% larger in diameter that the rotor [10]. These dimensions have been used to create the conventional Savonius type VAWT model. This model will be referred to as the baseline model hereafter. The 2D sketch of the blade profile has been shown in figure 1 (units in mm). The size of the flow domain has been selected from domain's dimensions independence study reported in a previous research work [11]. Hence, the flow domain has length x width x height of 17.6m x 17.6m x 12.7m.
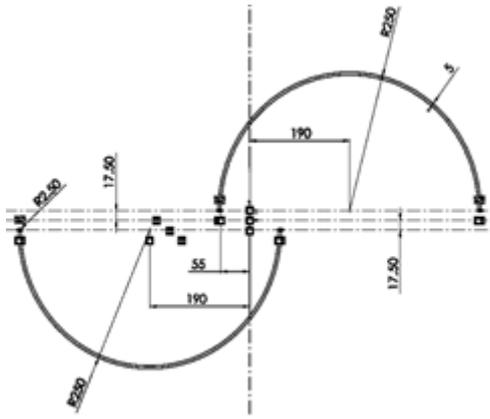
Figure 1. 2D sketch of the baseline blade

The flow domain has been meshed using unstructured tetrahedral mesh elements. The size of the mesh elements has been controlled using several mesh control functions. The global mesh sizing used for has minimum and maximum element sizes of 15mm and 400mm respectively. The rotational domain (comprising of the VAWT) has been refined using a local body sizing function of 200mm. The mesh on the blades' surfaces has been further refined using a face sizing function of 20mm. The resulting mesh has a total of 2,082,425 elements and 374,563 node points, shown in figure 2, and it meets the quality criteria, such as skewness, element quality, aspect ratio, Jacobian ratio and orthogonal quality.

Air turbulence in the vicinity of the VAWT has been modelled using the 2-equation Realizable k-ε turbulence model, where k is the turbulent kinetic energy and ε is the turbulent dissipation rate. This model performs well in case of flows exhibiting rapid strain, high pressure gradient, shear flows, moderate swirls and vortices [12], hence it suits the numerical modelling of VAWTs. In order to iteratively solve the Reynolds Averaged Navier-Stokes equations (RANS), for the incompressible and isothermal airflow around the VAWT, an inlet airflow velocity of 8m/sec has been specified, as it is the average annual wind speed at Huddersfield, UK. The air considered here has a constant density and dynamic viscosity of 1.225kg/m^3 and 1.7894x10^{-5} respectively.
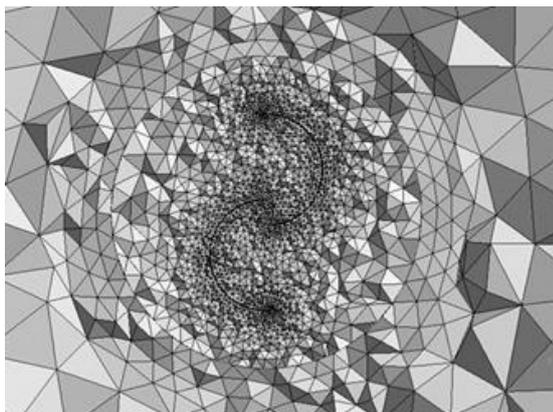

Figure 2. Mesh elements near the blades

The outlet boundary of the flow domain has been kept at atmospheric pressure condition. The rotation of the blades has been mimicked by incorporating sliding mesh between the stationary and the rotating zones. No-slip condition has been specified to the blade surfaces. A time step based numerical solver has been employed to run the steady flow of air around the VAWT. The time step size considered here corresponds to 3° rotation of the blades per time step, and has been shown in [13]

to be reasonable accurate for VAWTs. A statistically steady solution has been considered to be the convergence criteria for the numerical investigations.

3. Data Collection and Analysis

The mesh independence study has been conducted to determine the mesh size which provides a balance between the computational cost and the accuracy of the predicted results. For this purpose, four different meshes were generated with 1, 1.5, 2 and 2.5 million mesh elements. Revolution averaged torque and power coefficients (Cm and Cp) have been recorded. It can be seen in table 1 that when the mesh size increases from 1.5 to 2 million, the change in Cm and Cp are 0.5% and 0.7% respectively. Thus, the mesh having 1.5 million elements has been chosen for further analysis in the present study.

Table 1. Mesh independence results

No. of mesh elements	Cm	Cp
1,000,000	0.171	0.120
1,500,000	0.203	0.142
2,000,000	0.204	0.143
2,500,000	0.206	0.144

The same VAWT model has been considered in [2] for experimental investigations. The model showed peak Cp of 14.5%. Moreover, [14-16] also recorded similar values of peak Cp for the same VAWT model (around 14-15%). In the present study, numerical simulations have been run for a range of operating conditions i.e. TSR (λ) of 0.4-1 in order to estimate the peak Cp of the VAWT. Table 2 summarises the numerical results obtained; it can be seen that at λ=0.7, the VAWT model depicts peak Cp of 0.142 i.e. 14.2%, which is 2% less than that recorded in [10]. Hence, the numerical schemes used in the present study predict VAWT's performance characteristics with reasonable accuracy.

Table 2. Performance characteristics of the baseline VAWT

λ	Cm	Cp
0.4	0.304	0.122
0.5	0.260	0.130
0.6	0.230	0.138
0.7	0.203	0.142
0.8	0.175	0.140
0.9	0.141	0.127
1	0.107	0.107

The detailed local performance evaluation of the baseline model, and the subsequent tapered blade models, has been carried out at peak Cp point only (λ=0.7). Figures 3(a and b) depict the variations in static gauge pressure and flow velocity magnitude at the mid-plane along the height of the VAWT. It can be seen that the pressure is considerably higher on the windward side, with highest pressure at the tip of the returning blade. The pressure is lower on bottom leeward side of the VAWT, and is lowest on the suction side of the returning blade. Similarly, flow velocity has been noticed to be as high as 13.9m/sec on the suction side of the returning blade, and is considerably lower on the pressure side of

the same blade, and on the top leeward side of the VAWT. Some areas of flow recirculation have also been noticed downstream the VAWT.
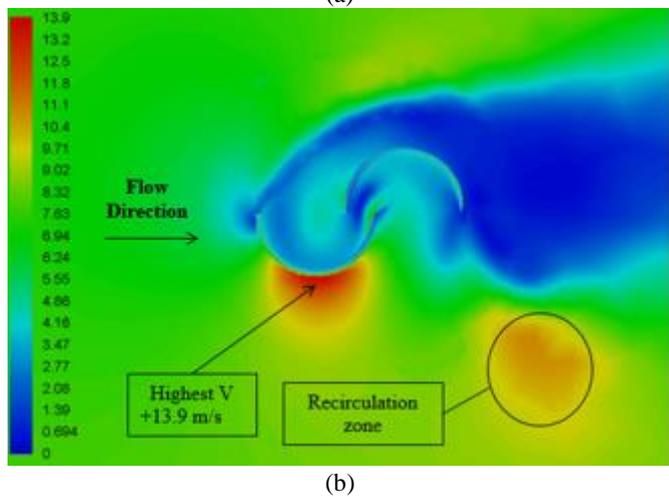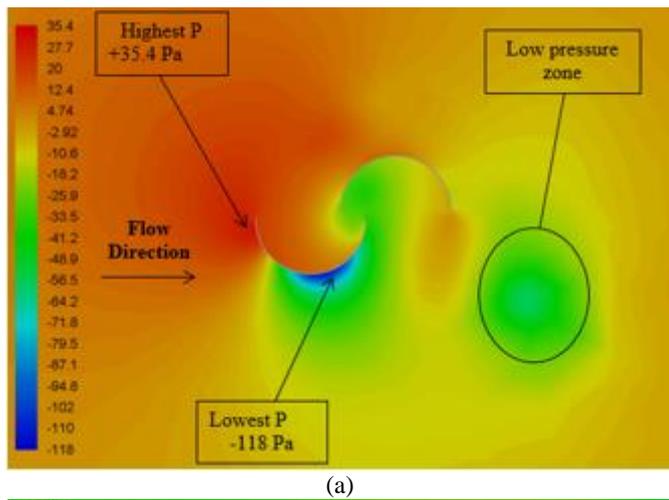

(a)

(b)

Figure 3. (a) Static pressure and (b) flow velocity variation in the vicinity of the baseline VAWT model

Figure 4 depicts the instantaneous variations in Cp and Cm of the baseline VAWT. Cyclic variations in both Cp and Cm are evident, where the number of cycles are equal to the number of blades of the VAWT. Same trends have previously been documented by other researchers [17-18]. It can be further seen that Cm reaches a value of 0.45, while Cp peaks at 0.32.
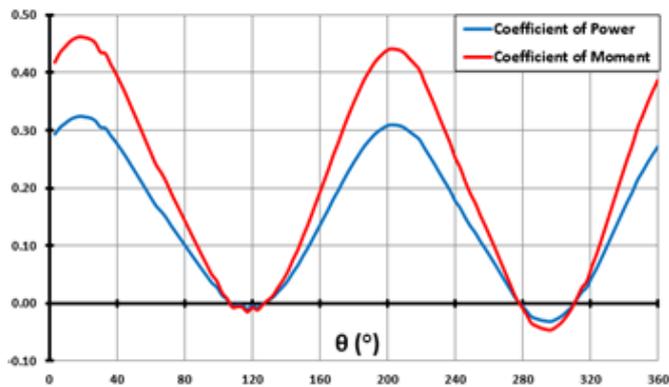

Figure 4. Instantaneous variation in Cp and Cm of the baseline VAWT

4. Results and Discussions

After analysing the local flow behaviour in the vicinity of the baseline VAWT, along-with the instantaneous performance of the blades, detailed discussions on the effects of blade tapering is reported here. In the present study, three different VAWT configurations with various blade tapering have been analysed. These designs correspond to Delta, Rhomb and Cross shaped blades, as shown in figure 5. The overlap and gap ratios have been kept constant, meaning that where the blade profile reduces in size, the gap and overlap distances are reduced proportionally to keep these ratios same.
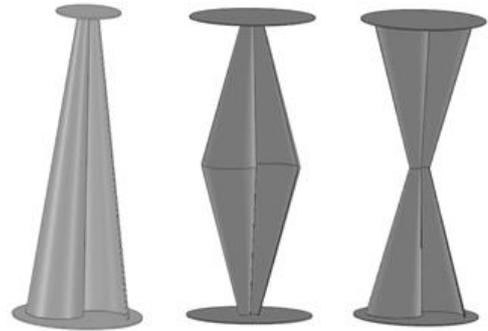

Figure 5. Tapered blade configurations of the VAWT (a) Delta, (b) Rhomb and (c) Cross

It is clear that the swept area and the rotor radius of these configurations are different to the baseline model. Hence, the swept areas and the rotor radii have been computed for accurate estimation of Cp and Cm of these VAWT models. The mean rotor radius (Rm) has been calculated based on the radii of the smaller blade side (Rs) and the bigger blade side (Rb); example of delta shaped blades has been shown in figure 6.
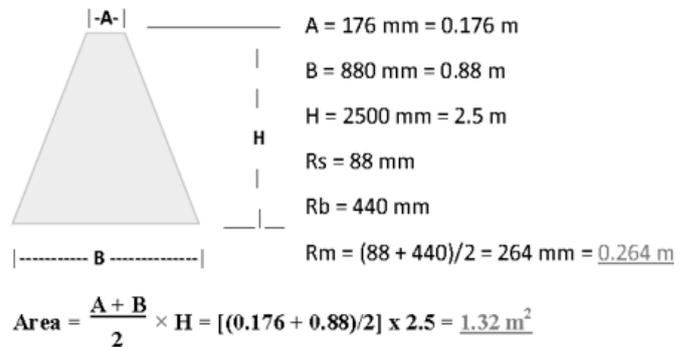

Figure 6. Calculation of the mean rotor radius and the swept area of the Delta rotor
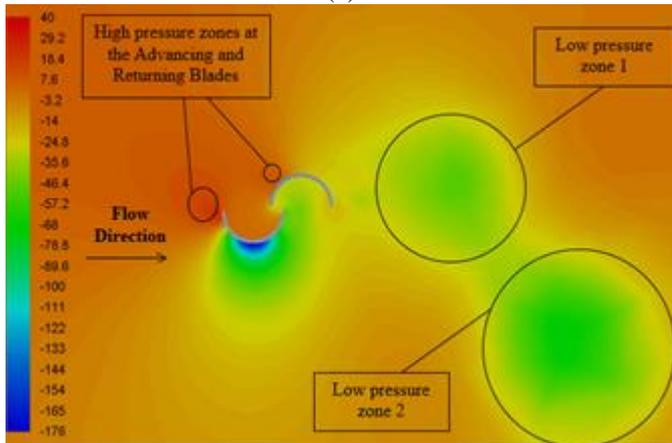
Figure 7 depicts the variation in static gauge pressure in the vicinity of the three tapered blade considered. The scale of the pressure distributions has been kept the same for all the three models for effective comparison purposes. It can be seen that for the Delta shaped model, the low pressure zone downstream the VAWT is bigger than the one for the Rhomb shaped model. It can also be seen that the Rhomb shaped model has larger high pressure zones, acting on both advancing and returning blades, compared to the Delta shaped and Cross shaped models. Upon careful examination, it can be noticed that the size of the high and low pressure zones is more disproportionate in Rhomb shaped model than the Delta shaped model. It can be further noticed for the Cross shaped model that there are two low pressure zones downstream the VAWT, which indicates that as the blades grow in size from the centre, the flow non-uniformity downstream the VAWT increases considerably.
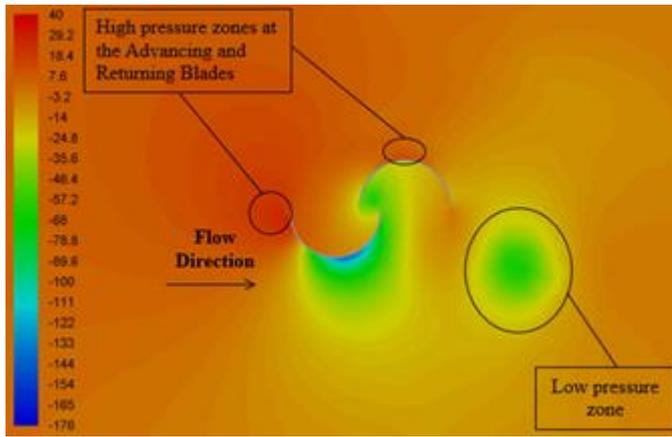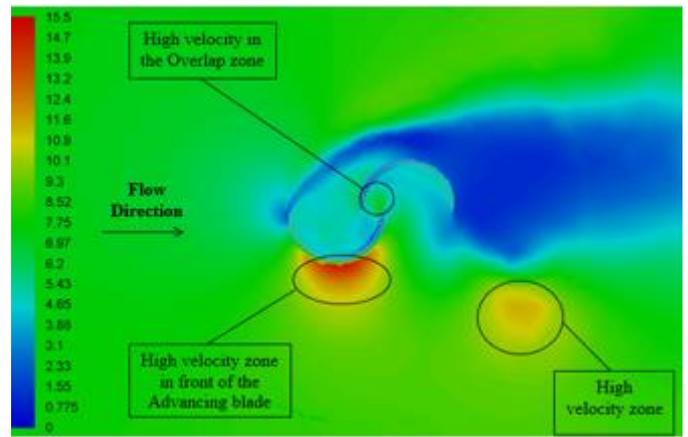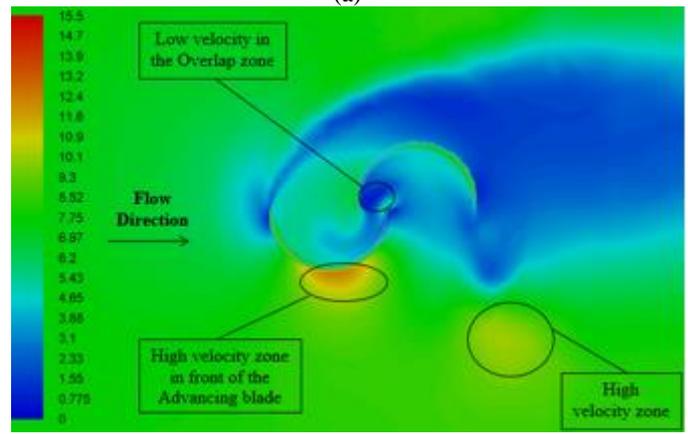
(a)
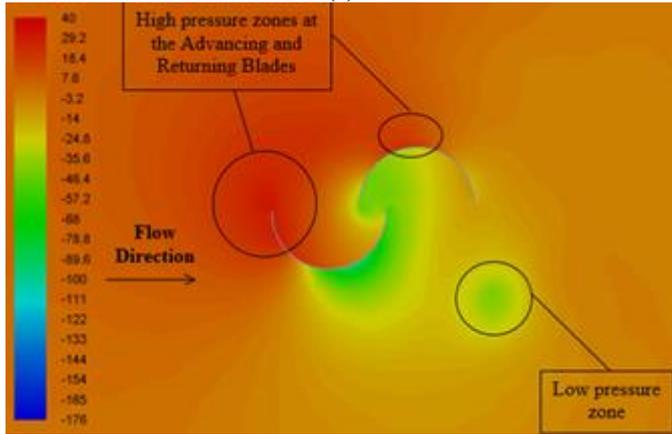
(b)

(c)

Figure 7. Static pressure variations in the vicinity of the tapered VAWTs (a) Delta (b) Rhomb (c) Cross

(a)

(b)

(c)

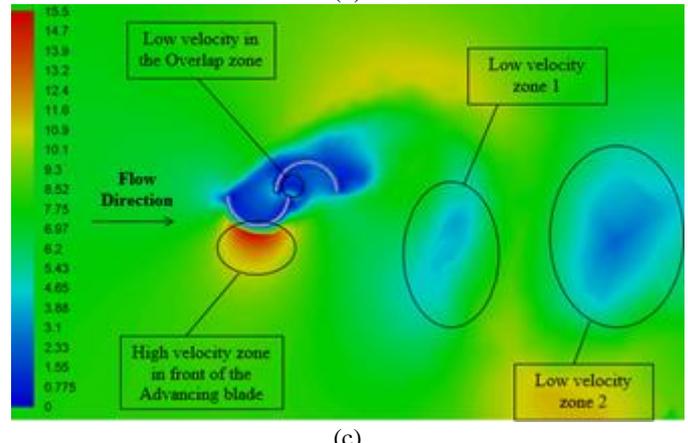**Figure 1.** Flow velocities variations in the vicinity of the tapred VAWT (a) Delta (b) Rhomb (c) Cross

Figure 8 depicts the variation in the flow velocity magnitude in the vicinity of the three tapered blade models considered. It can be seen that for the Delta shaped model, the high velocity zone on the suction side of the advancing blade is significantly bigger than for the Rhomb shaped model. It can also be seen that for the Rhomb shaped model, the velocity in the overlap zone is lower than for the Delta shaped model. Moreover, it can be further noticed that the high velocity zone on the suction side of the advancing blade in the Delta shaped model is similar to the one for the Cross shaped model, however, the Cross shaped model does not depict the high velocity region in the overlap zone.

The variations in the time dependent coefficients of power and torque, during one complete revolution of the VAWTs, have been depicted in figure 9. It can be clearly seen that all the three tapered blade VAWT models show similar cyclic variations, but the Delta shaped model exhibits higher instantaneous, as well as revolution averaged coefficients of power and torque, summarised in table 3. Hence, the Delta shaped tapered blades perform better than the Rhomb and Cross shaped tapered blades in VAWTs. Upon comparing tables 3 and 2 (at λ=0.7), it is evident that the average performance coefficients of the tapered blade VAWTs are lower than the baseline VAWT model. This means that tapering of a VAWT's blades has an adverse effect on the performance of the VAWT. Between the three tapered blade models, it has been shown that the Delta shaped model is more efficient than the rest of the two tapered blade models.
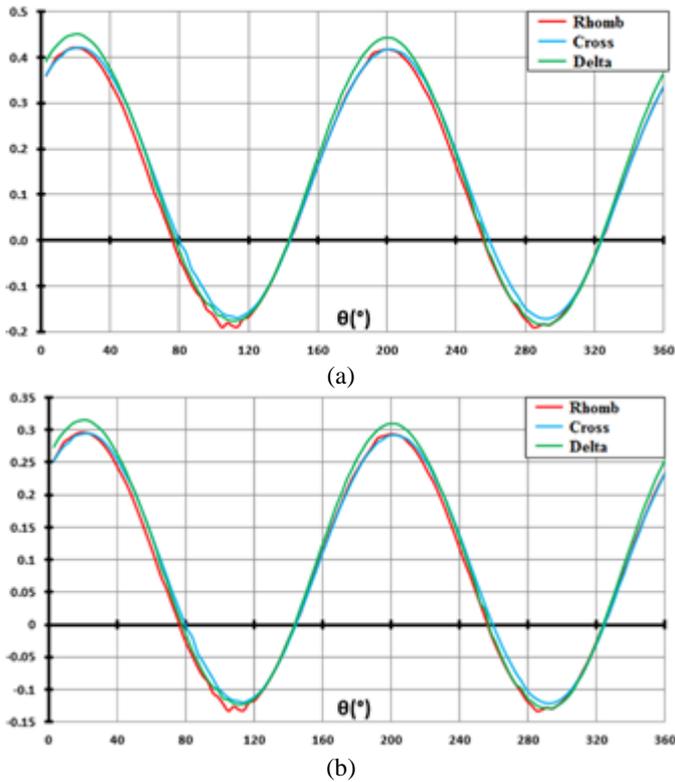
(a)

(b)

Figure 2. Instantaneous variation in (a) Cp and (b) Cm for the tapered blade configuration of the VAWT

Table 3. Revolution average Cp and Cm of the tapered blade VAWTs

Blade Shape	Average Cp	Average Cm
Delta	0.129	0.120
Rhomb	0.114	0.142
Cross	0.127	0.143

Further analyzing the reasons for lower efficiency of the Delta shaped model in particular, figure 10 depicts the static gauge pressure variations on the VAWT model comprising of Delta shaped blades.
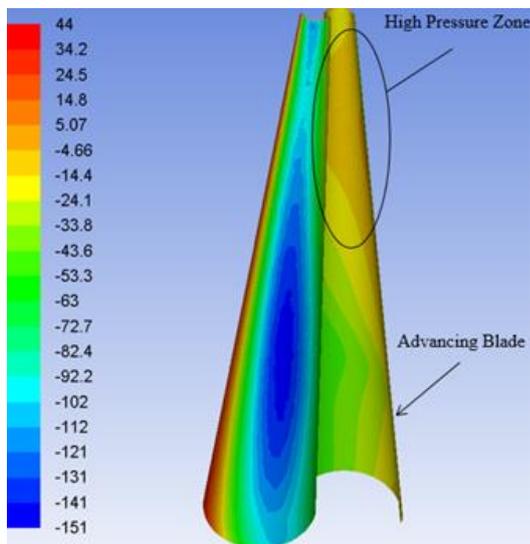

Figure 10. Static Pressure Variation of the blades of the Delta shaped design

It can clearly be seen that the high pressure zone exists only at the top of the advancing blade, where the relative aspect ratio is higher, whereas the low aspect ratio region depicts lower pressure. The overall lower efficiency in Delta shaped blades is due to the fact that 66.7% of the VAWT's swept area is in the lower aspect ratio region. This means that 66.7% of the VAWT is working at lower efficiency than the baseline model. Calculations in figure 11 show the area calculation for Delta shaped blades.
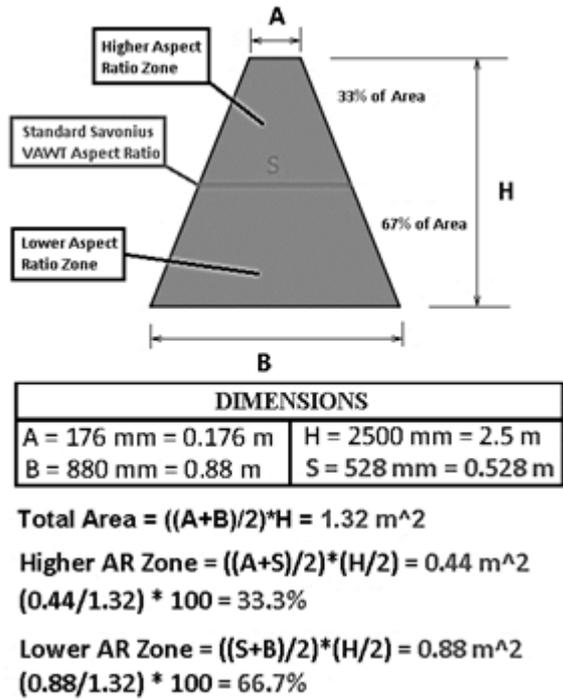

DIMENSIONS	
A = 176 mm = 0.176 m	H = 2500 mm = 2.5 m
B = 880 mm = 0.88 m	S = 528 mm = 0.528 m

Total Area = ((A+B)/2)*H = 1.32 m^2

Higher AR Zone = ((A+S)/2)*(H/2) = 0.44 m^2
(0.44/1.32) * 100 = 33.3%

Lower AR Zone = ((S+B)/2)*(H/2) = 0.88 m^2
(0.88/1.32) * 100 = 66.7%

Figure 11. Calculation of the swept area of the Delta shaped blades with respect to aspect ratio

Local torque generation from the Delta shaped blades is shown in figure 12. It can be seen that the torque contribution from the higher aspect ratio region is 29.95%, while it is 70.05% from the lower aspect ratio region. This is consistent with the explanation based on the swept area above.
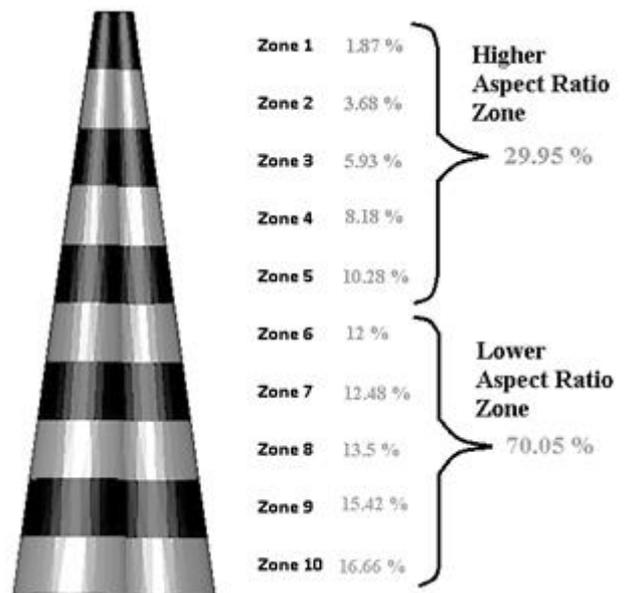

Figure 12. Local torque contributions from Delta shaped blades

5. Conclusion

The efficiency of a wind turbine is directly affected by the shape of the blades it has. The effects of blade tapering on the performance characteristics of a Savonius VAWT have been numerically investigated. For this purpose, three blade shapes, with different tapering, have been considered, namely Delta, Rhomb and Cross shaped blades. The results obtained for these blades have been compared against the conventional blade shape.

It can be concluded form the results obtained that the performance characteristics of a VAWT reduces by the introduction of blade tapering. The primary reason for this has been shown to be the fact that 70% of the blades work at lower aspect ratio, and hence lower efficiency, while the remaining 30% of the blades work at higher aspect ratio and efficiency. The overall efficiency reduces compared to conventional blade shape because the higher efficiency zones do not fully compensate for the lower efficiency zones. The Delta shaped blades have shown to be performing superior compared to the Rhomb and Cross shaped blades, again due to the aforementioned reasons.

References

[1] Hara, Y. Sumi, T. Wakimoto, M. Kogo, S. Mizuguchi, S. Yoshimi, K. and Akimoto, H. (2014). Comparison between symmetrical and cambered blade sections for small-scale wind turbines with low center of gravity. JSME Journal of Fluid Science and Technology. Volume: 9. 1 – 16.

[2] Asim, T. Oliveira, A. Charlton, M. and Mishra, R. (2019). Improved Design of a Multi-Stage Continuous-Resistance Trim for minimum Energy Loss in Control Valves. Energy. Volume: 174. 954 – 971.

[3] Asim, T. Oliveira, A. Charlton, M. and Mishra, R. (2019). Effects of the Geometrical Features of Flow Paths on the Flow Capacity of a Control Valve Trim. Petroleum science and Engineering. Volume: 172. 124 – 138.

[4] Asim, T. Algadhi, A. and Mishra, R. (2018). Effect of Capsule Shape on Hydrodynamic Characteristics and Optimal Design of Hydraulic Capsule Pipelines. Journal of Petroleum Science and Engineering. Volume: 161. 390 – 408.

[5] Asim, T. Charlton, M. and Mishra, R. (2017). CFD based Investigations for the Design of Severe Service Control Valves used in Energy Systems. Energy Conversion and Management. Volume: 153. 288 – 303.

[6] Asim, T. and Mishra, R. (2017). Large Eddy Simulation based Analysis of Complex Flow Structures within the Volute of a Vaneless Centrifugal Pump. Sadhana. Volume: 42. 505 – 516.

[7] Asim, T. and Mishra, R. (2016). Optimal design of hydraulic capsule pipelines transporting spherical capsules. Canadian Journal of Chemical Engineering. Volume: 94. 966 – 979.

[8] Asim, T. and Mishra, R. (2016). Computational Fluid Dynamics based Optimal Design of Hydraulic Capsule Pipelines Transporting Cylindrical Capsules. International Journal of Powder Technology. Volume: 295. 180 – 201.

[9] Asim, T. Mishra, R. Abushaala, S. and Jain, A. (2016). Development of a Design Methodology for Hydraulic Pipelines Carrying Rectangular Capsules. International Journal of Pressure Vessels and Piping. Volume: 146. 111 – 128.

[10] Alexander, A.J. and Holownia, B.P. (1978). Wind Tunnel Test of a Savonius Rotor. Journal of Industrial Aerodynamics. Volume: 3. 343 – 351.

[11] Mohamed, M.H.A. (2010). Design Optimization of Savonius and Wells Turbines, MSc thesis, University of Magdeburg, Germany.

[12] Asim, T. Mishra, R. Ubbi, K. and Zala, K. (2013). Computational fluid dynamics based optimal design of vertical axis marine current turbines, Procedia CIRP. Volume: 11. 323 – 327.

[13] Park, K. Asim, T. and Mishra, R. (2015). Numerical Investigations on the Effect of Blade Angles of a Vertical Axis Wind Turbine on its Performance Output. International Journal of COMADEM. Volume: 18. 3 – 10.

[14] Fernando, M.S. (1987). On the Performance and Wake Aerodynamics of the Savonius Wind Turbine, PhD thesis, University of British Columbia, Canada.

[15] Aldoss, T. and Kotb, M.A. (1991). Aerodynamic Loads on a Stationary Savonius Rotor. JSME International Journal. Volume: 34. 52 – 55.

[16] Fujisawa, N. and Gotoh, F. (1992). Visualization study of the flow in and around a Savonius rotor. Experiments in Fluids. Volume: 12. 407 – 412.

[17] Shahzad, A. Asim, T. Mishra, R. and Paris, A. (2013). Performance of a Vertical Axis Wind Turbine under Accelerating and Decelerating Flows. Procedia CIRP. Volume: 11. 311 – 316.

[18] Asim, T., Mishra, R., Kaysthagir, S., and Aboufares, G., (2016), Performance Comparison of a Vertical Axis Wind Turbine using Commercial and Open Source Computational Fluid Dynamics based Codes in proc. International Conference on Jets, Wakes and Separated Flows, 16-18 June, Stockholm, Sweden.